Supplement of Earth Surf. Dynam., 10, 457–471, 2022
https://doi.org/10.5194/esurf-10-457-2022-supplement

Earth Surface Dynamics
Open Access
EGU

Supplement of

Climate changes and the formation of fluvial terraces in central Amazonia inferred from landscape evolution modeling

Ariel Henrique do Prado et al.

Correspondence to: Ariel Henrique do Prado (ariel.doprado@geo.unibe.ch)

SUPPLEMENTARY MATERIAL

S1 NUMERICAL MODEL IMPLEMENTATION AND NUMERICAL SOLUTIONS

S1.1. Discretization of the surface

In numerical models, the discretization of the surface is usually done by the division of the topography into cells, which are small portions of area represented by an array with information such as coordinates, area and height. Two common approaches to define the shape of the cells are: (1) a regular grid with square cells, with the disadvantage of the limited possible directions between connected cells, causing artificial symmetries (e.g. Beaumont 1992, Van De Wiel et al. 2007), and (2) irregular grids formed by Voronoi cells, which eliminate the artificial symmetry observed in regular grids but increase the computational memory necessary to allocate the information about the shape of each cell (e.g. Sacek, 2014).

To overcome the above disadvantages, the SPASE model uses a regular hexagonal grid to represent the surface (Fig. S1). The main reason for doing so is the necessity of controlling the length of the cell's sides, because the width of a river inside a cell needs to be smaller than the margin of the cell into which the stream is flowing. This condition is required in order to guarantee only one flow direction. Additionally, the regular hexagonal grid gives six possible flow directions instead of four as is the case for quadratic cells.

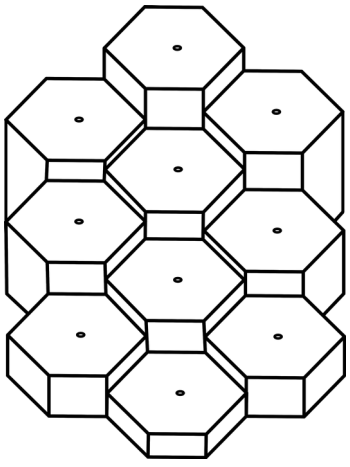

Figure S1 Example of regular hexagonal grid in 3D.

Figure S2 shows the SPASE model work flow chart. The first step is the definition of the geometric parameters, such as the size and the number of grid cells, and the parameters of the governing equations of the surface processes. The creation of a regular hexagonal grid requires specific parameters, such as the length of the cell margin and the number of cells in the x and y axes.

The grid is created after the definition of the parameters, and each cell is classified in three types: (1) Inner cells, located inside the grid. Such cells have six neighboring cells and are subject to all Earth surface processes of the model. (2) Edge cells, located on the edge of the grid. These cells can receive fluvial input of sediment and water from outside of the grid and are also subject to all Earth surface processes. (3) Sink cells, located on the edge of the grid. They are defined as cells whose height values do not vary over time. They receive water and sediment discharge that is derived from the model. These cells are used to control the base level of the model.

Any topography discretized into a hexagonal grid can be used as input in the model as the initial topography, in a way that the height value of each cell represents the average heights in the cell area.

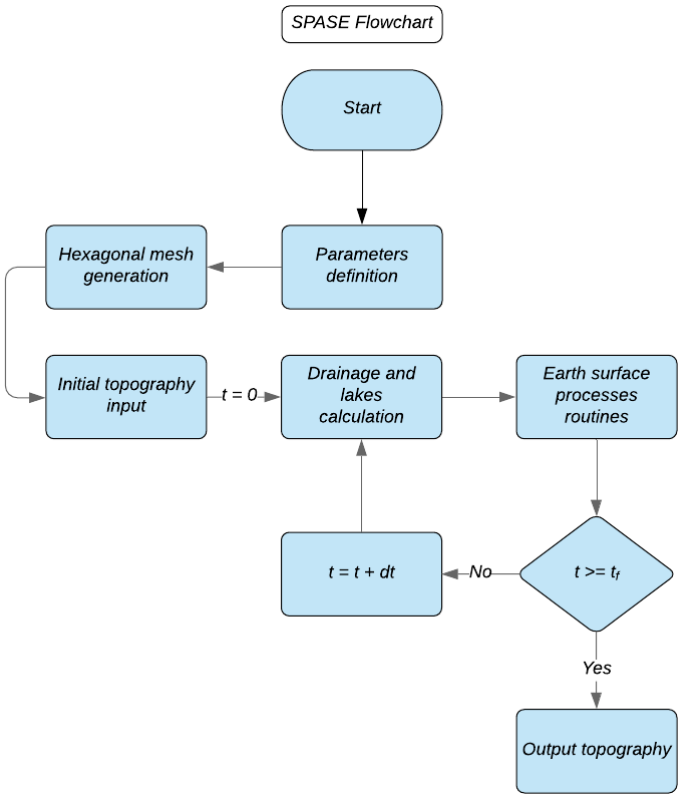

Figure S2 Flowchart of SPASE. The time is counted by the variable t , the time step is defined by dt and the total time of modelling is t_f .

S1.2 Earth surface drainage and lakes

In SPASE, groundwater flow is not considered, so all volumes of input water including the contribution of rainfall has to exit through the sink cells, thereby ensuring the conservation of water mass. The calculation of the surface drainage network is accomplished in a similar way to the cascade algorithm presented by Braun and Sambridge (1997). Rainfall is considered as high as 3000 mm/year, which is an approximation of the regional average (Espinoza et al, 2009a), whereas the *runoff coefficient* (Effective proportion of rainfall) is set to 50%, following Guimberteau et al. (2013).

Since the length of the cell margins in the model is larger than the width of the channels within the cells, the water flow direction is always defined as the direction to the lowest neighbor. Thus, in all cells the volume of water, due to the rainfall rate and the water input from outside of the grid, is transferred to the lowermost neighbors thereby forming the drainage network (Fig. S3).

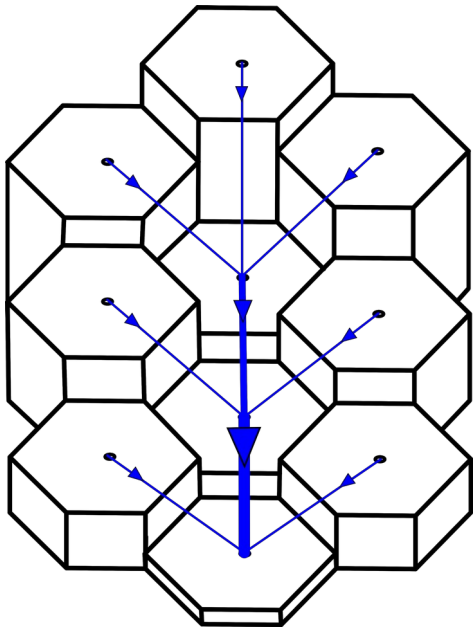

Figure S3 Example of a drainage network in hexagonal grid. Blue lines represent the drainage where the thickness is relative to its discharge and the arrows indicate the direction of water flow.

The first step to calculate the drainage pattern comprises a sorting of the cells from highest to lowest. After this step, the flow direction in each cell is defined by the location of the lowest neighbour (Fig. S4). In cases where a given cell does not have a neighbouring cell with a lower elevation, it becomes a local minimum resulting in the formation of a lake.

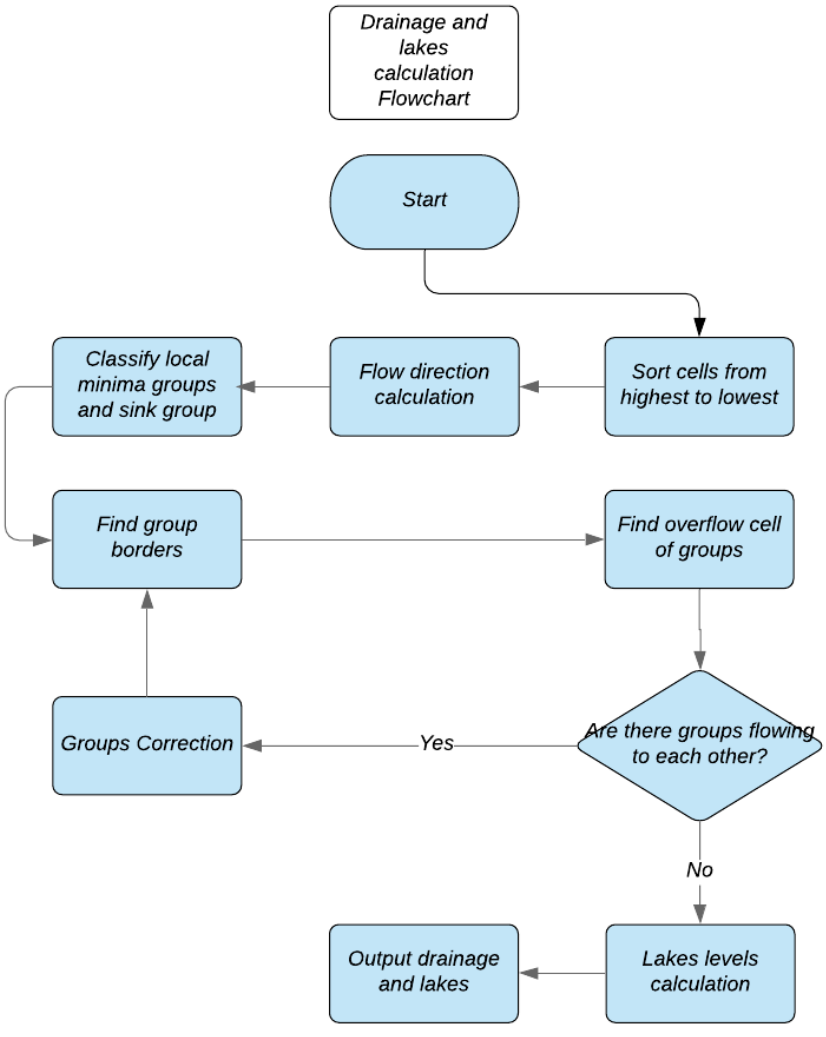

Figure S4 Flowchart illustrating how the drainage network and the lakes are calculated.

During the process where the flow direction is calculated, the local minima and the sink cells are flagged. After that, each cell in the grid is classified as belonging to a group of cells where the water flows to the same local minimum or to the same sink cell (sink group). In each group, every cell that has a neighbour which does not belong to the group is then classified as a group border cell.

Lakes are formed in groups of local minima that accumulate water until they reach the necessary height to overflow to a neighbouring cell with a lower elevation, which then is referred to as an overflow cell. Therefore, the overflow cell will always belong to a neighbour group, with the exception of sink groups where the overflow cell is the sink cell itself. To define the overflow cell, all border cells of a group with local minima are sorted from lowest to highest, and their heights are placed in an array (B_{group}). For each cell in the array B_{group}, the

height of the lowest neighbour in an external group is stored in an array (S_{neigh}). The overflow cell is therefore defined by the following algorithm:

```
N = 0
Flag = 0
Smaller = S_neigh[N]
while Flag == 0:
    if Smaller > S_neigh[N]:
        Smaller = S_neigh[N]
    if S_neigh[N] <= B_group[N+1] and S_neigh[N] <= Smaller:
        Flag = 1
        The address of S_neigh[N] is the overflow cell of the group
        continue
    if S_neigh[N] > Smaller and Smaller <= B_group[N+1] :
        Flag = 1
        The address of Smaller is the overflow cell of the group
        continue
    N = N + 1
    if N > N_total :          # N_total is the total number of border cells
        Flag = 1
        The overflow cell of the group is the address of Smaller
        continue
```

After this routine, the drainage network linking the groups is calculated. To avoid cases of groups where water flows to each other thereby forming a loop, a routine is called that accomplishes a correction where the corresponding groups are merged to a 'supergroup'. This 'supergroup' is treated as a group and undergoes the same process of *finding border cells* and *overflow cells* as described above. This step is repeated until all groups are connected to a sink group (Figure S4).

After the drainage network and all the overflow cells have been calculated, lake cells are defined as those cells in a group where the elevations are lower than the *lake height* of the same group. The *lake height* is defined as: (i) the height of the overflow cell, where the neighbouring border cells of the overflow cell are lower than the overflow cell itself, or (ii)

the height of the lower border cell, i.e., the neighbour of the overflow cell, where the neighbor border cells of the overflow cell are higher than the overflow cell itself. The depth of the lake in a lake cell is defined by the difference between the cell height and the *lake height*.

The discharge in each cell is calculated after the flow directions and lake cells are defined. When the flow direction leads to a lake cell, the entire water flux is transferred to its overflow cell, and the sediment is deposited in the first lake cell.

S1.3 Formulation of the Earth surface processes in the hexagonal grid

This section describes how the depositional and erosional processes are considered in the model, and how the model is set up such that the formation of terraces is possible. This requires the introduction of new geometrical parameters inside the cells.

Since the channel width that passes through a cell cannot be greater than the length of the corresponding cell edge, it follows that the channel area ($A_{channel}$) is always smaller than or equal to the total cell area (A_{hex}). Considering the case where incision occurs within a cell, a fraction of the cell area $A_{channel}$ will experience erosion, and the rest of the same cell $A_{terrace}$ will constitute a terrace that forms in this particular cell. Accordingly, the area of terrace ($A_{terrace}$) is the difference between A_{hex} (i.e. the original cell) and $A_{channel}$. The occurrence of lateral erosion inside a cell results in an increase of the area of the floodplain ($A_{floodplain}$) which is then larger than or equal to $A_{channel}$, with initial value defined as equal to $A_{channel}$. Accordingly, there are two heights associated with each of these areas. These are the terrace height ($h_{terrace}$) and the channel height ($h_{channel}$), which is also the floodplain height and which is therefore used to define the flow direction. Table S1 shows the geometric variables that are used for the calculation of the surface processes in each cell.

Using the relationships between water discharge and channel width in Amazonia based on data available through the Brazilian Water Agency (A.N.A.), we can predict the width of a channel for a given discharge (Figure S5 and Table S2). Under the assumption that the channel is straight within a cell, $A_{channel}$ is calculated as the product of the width of the channel in the cell and the distance between the center of two cells (L_{cell}).

Table S1 Geometrical parameters of a cell that are used to calculate the Earth surface processes.

A_{hex}	Area of a hexagonal cell
$A_{channel}$	Area of channel
$A_{terrace}$	Area of terrace
$A_{floodplain}$	Area of floodplain (>= $A_{channel}$)
$h_{channel}$	Height of channel and floodplain
$h_{terrace}$	Height of terrace
L_{cell}	Distance between the center of two regular hexagonal cells

We labelled the channel cells according to their elevations $h_{channel}$, which we then used as a constraint to define the flow direction (see above). We use this pattern to define the order through which the calculations of erosion, deposition etc. proceed in the model. Accordingly, the volume of sedimentary input (q_{sed}) is calculated for each cell following this order, where q_{sed} [L^3] is the sum of the external input of sediment from cells located above or from outside of the grid and the volume of sediment resulting from lateral erosion within the cell itself. In the same order, we also consider the volume of sediment eroded from or deposited on the channel bottom (see main text for criteria). After this process is applied in all cells, the *Earth surface processes routine* stage ends (Figure S2).

S1.4 Discretization of lateral erosion

This section describes how the lateral erosion is accomplished in each cell of the model. Inside the model, this process was calculated for cells containing rivers with water discharge above 1000 m^3/s.

If $h_{channel}$ is lower than $h_{terrace}$ in a cell, lateral erosion takes place, and the volume of the eroded sediment, B, is calculated through the integrated form of equation 4.3 in the main text:

$$B = a_{le}\left[\left(h_{terrace} - h_{channel}\right) + h_{depth}\right] \quad \text{(S1.1)}$$

where for simplicity h_{depth} is defined as the width of channel divided per 100 for rivers with

discharge above 1000 m^3/s, which is acceptable for high discharge rivers following the relationship proposed by Moody and Troutman (2002). Finally, a_{le} is the discretized form of equation 4.4 in the main text, defined by:

$$a_{\mathrm{le}} = r \,.\, \alpha_1 \,.\, q_{eqb}^{\alpha_2} \frac{A_{channel}}{A_{floodplain}} \tag{S1.2}$$

where, q_{eqb} is the carrying capacity of the channel [$L^3\ T^{-1}$] defined in S1.3, $\alpha_1$and $\alpha_2$are the lateral erosion coefficients, which depend on the erosional resistance of the lateral margins of the channels. The random fraction coefficient (*r)* is a random value between 0 and 1 in a uniform distribution. It is introduced in the equation with the intention to take into account the complex effects caused by the hydrodynamic conditions that eventually causes the lateral erosion to occur at higher or lower rates. The ratio between $A_{channel}$ and $A_{floodplain}$ quantifies how the conditions of a influences the process of lateral erosion and the formation of a terrace level inside a cell. In particular, a low $A_{floodplain} / A_{channel}$ ratio yields a relatively small amount of lateral erosion within a cell during a timestep.

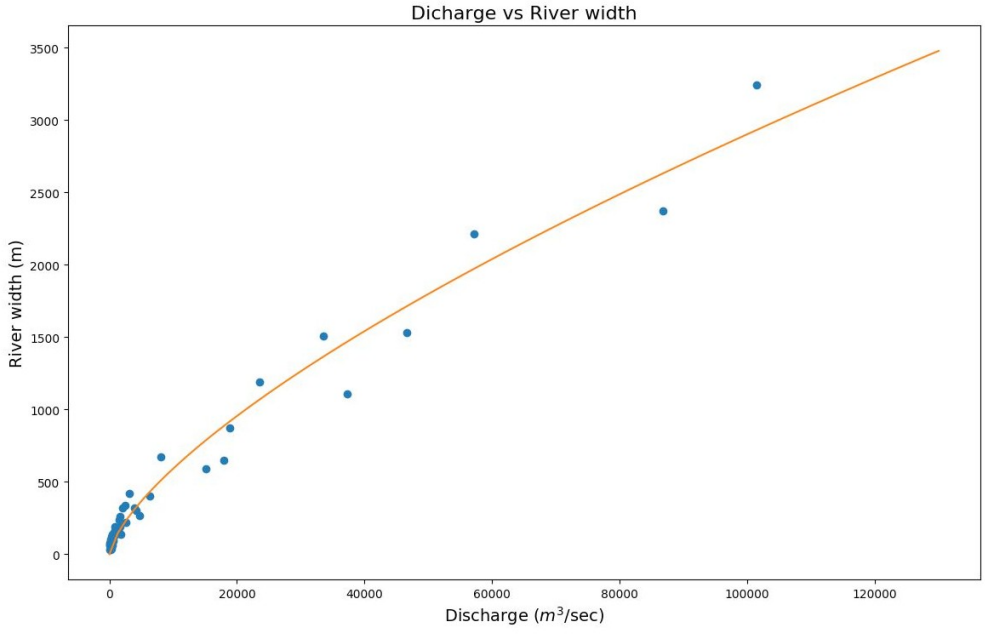

Figure S5 Empirical relationship between mean water discharge and river widths in Amazonia. Blue dots are the empirical data from 57 data points in 24 amazonian rivers, obtained from Brazilian Water Agency (A.N.A.). Orange line is the exponential curve fitted to the data.

Table S2 Annual mean water discharge and width of Amazonic rivers at gauging stations. Data obtained from Brazilian Water Agency (A.N.A.).

River - Station	Mean Discharge (m^3/s)	Width (m)
Acre - Assis Brasil	62	80
Acre- Brasileia	126	50
Acre - Floriano Peixoto	631	90
Acre - Rio Branco	376	70
Acre - Xapuri	204	60
Coari - Seringal Moreira	285	100
Curuca - Santa Maria-Flores	986	140
Envira - Feijo	446	120
Envira - Seringal Santa Helena	332	120
Gregorio - Fazenda Paranacre	48	70
Gregorio - Seringal Santo Amaro	200	70
Guapore - River Watch	3087	420
Iaco - Seringal Sao Jose	238	60
Itacuaí - Ladário Jusante	1680	190
Itui - Ladario	720	150
Itui - Seringal DoItui	781	150
Ituxi - Jurene	478	60
Javari - Estirão Do Repouso	2610	220
Javari - Palmeiras Do Javari	634	100
Juruá - Cruzeiro Do Sul	922	180
Juruá - Eirunepé Montante	1822	140
Juruá - Foz Do Breu	174	70
Juruá - Gavião	4741	270
Juruá - Ipixuna	1352	170
Juruá - Santos Dumont	4178	300
Juruá - Thaumaturgo	413	120
Jutaí - BarreiraAlta	1642	260
Jutaí - Colocação Caxias Novo	486	130
Jutaí - Conceição - Ilha Nova Da Sorte	815	190
Jutaí - Porto Seguro	2457	340
Liberdade - Seringal Bom Futuro	89	60
Madeira - Abuna	17951	650
Madeira - Fazenda Vista Alegre	33588	1510
Madeira - Porto Velho	18843	870
Madeira - Manicore	23506	1190
Moa - Serra Do Moa	32	30
Mamore - Guajara-Mirim	7999	670
Mucuim - Cristo	266	40
Pauini - Fazenda Borangaba	821	160
Purus - Aruma	15079	590
Purus - Canutama	6369	400
Purus - Manoel Urbano	795	160
Purus - Santa Rosa Do Purus	455	100
Purus - Seringal Caridade	1362	160

River - Station	Mean Discharge (m^3/s)	Width (m)
Purus - Seringal Fortaleza	3919	320
Purus - Valparaiso Montante	2109	320
Solimões - Itapeua	86767	2370
Solimões - Manacapuru	101463	3240
Solimões - SantoAntonioDoIca	57216	2210
Solimões - São Paulo De Olivenca	46635	1530
Solimões - Tabatinga	37344	1110
Tapaua - Bacaba	1523	240
Tarauaca - Envira	1215	170
Tarauacá - Seringal São Luiz	150	100
Tarauacá - Tarauacá Jusante	424	140
Tefé - Estirão Da Santa Cruz	544	120
Tefé - Fazenda Boa Esperanca	171	30

The maximum volume of sediment that a river can carry during a timestep Δt within a given cell (q_{eqb}) is calculated through integrating Eq. 1 in the main text and is given by:

$$q_{eqb} = K_f \cdot \Delta t \cdot Q_r^{\,m} \cdot \left(\frac{h_i - h_j}{L_{cell}}\right)^n \quad \text{(S1.3)}$$

where Q_r is the water discharge in the cell due to rainfall and external input, h_i is the $h_{channel}$ of the actual cell and h_j is the $h_{channel}$ of the cell into which the model river will flow. Fig. S6 shows an example of lateral erosion occuring in a hexagonal grid.

If the entire terrace area is eroded inside a cell ($A_{terrace}$ = 0; $A_{floodplain}$ = A_{hex}), lateral erosion takes place in its neighbouring cells only when the neighbouring cells have a $h_{channel}$ that is greater than the $h_{channel}$ of the original cell. The volume of sediment that is eroded in each neighbouring cell is calculated using Eq. S1.1. In this case, $h_{terrace}$ is the terrace height of a neighbouring cell and $h_{channel}$ is the channel height in the original cell. The total volume of laterally eroded sediments (inside a cell + neighbour cells) is added to the q_{sed} of the original cell.

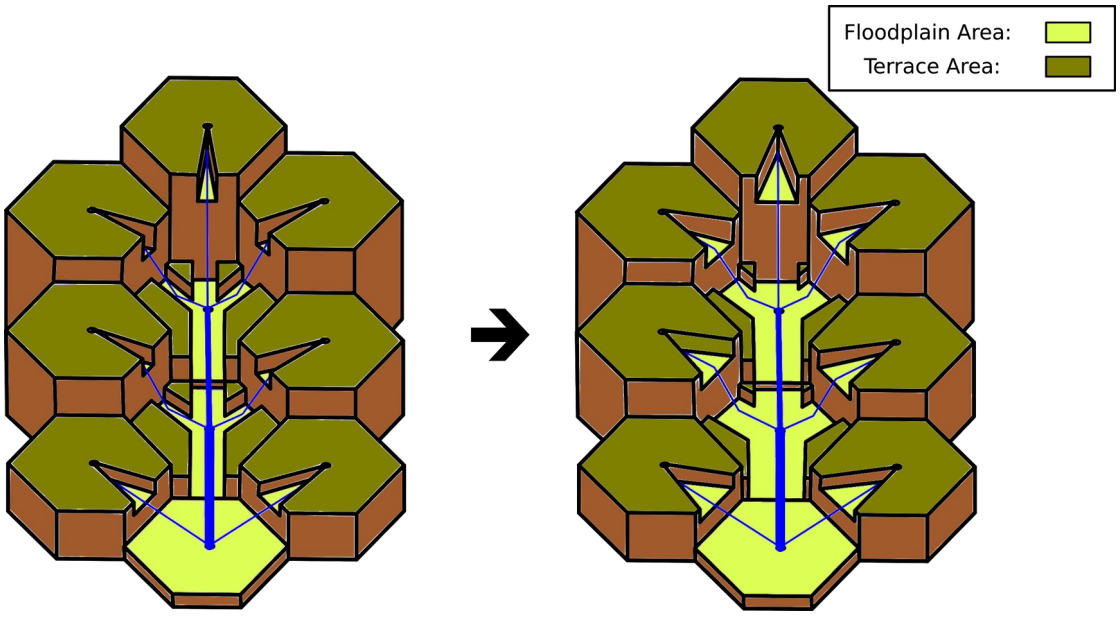

Figure S6 Conceptual model representing the situation before and after the occurrence of lateral erosion in a hexagonal grid during one time step. Each cell has three geometrical parameters, channel area in blue ($A_{channel}$), floodplain area in light green ($A_{floodplain}$) and terrace area in dark green ($A_{terrace}$). After the corresponding time step, the floodplain area in each cell increases in response to lateral erosion.

S1.5 Transport, deposition and bed erosion by fluvial processes

The difference between q_{sed} and the q_{eqb} (Eq. S1.3) that is calculated in the cell determines whether a cell experiences deposition or erosion. If $q_{sed} > q_{eqb}$, deposition takes place and Eq. 2 in the main text will take the following discrete form:

$$\Delta h_{channel} = \frac{q_{sed} - q_{eqb}}{A_{floodplain}} \quad \text{(S1.4)}$$

Where $\Delta h_{channel}$ is the value that will be added to $h_{channel}$ of the cell. The length scale of the material in suspension (L_s) in the river is considered as equal to 1, not appearing in this equation. If $h_{channel} + \Delta h_{channel}$ is greater than the $h_{terrace}$ of the cell, the following equation is solved:

$$\Delta h_{terrace} = \frac{[q_{sed} - q_{eqb} - A_{floodplain} \cdot (h_{terrace} - h_{channel})]}{A_{hex}} \quad \text{(S1.5)}$$

where $\Delta h_{terrace}$ is the height that will be added to the initial $h_{terrace}$ of the cell. After $\Delta h_{terrace}$ is calculated, the variables are updated as follows: $h_{terrace} = h_{terrace} + \Delta h_{terrace}$; $h_{channel} = h_{terrace} + \Delta h_{terrace}$; $A_{floodplain} = A_{hex}$. After the calculation of sediment deposition with S1.4 or if necessary S1.5, the volume q_{eqb} is transferred to the q_{sed} in the neighbouring cell that receives

the water and sediment.

If $q_{sed} < q_{eqb,}$ bed erosion takes place and Eq. 2 takes the following discrete form:

$$\Delta h_{channel} = \frac{q_{sed} - q_{eqb}}{A_{channel}} \frac{L_{cell}}{L_a} \quad \text{(S1.6)}$$

where $\Delta h_{channel}$ is the height that will be subtracted from the initial $h_{channel}$. The length scale of the river bed material (L_a) represents a value that is considered to be constant for all cells, since the landscape represents an alluvial environment with recent deposits. The ratio between L_{cell} and L_a needs to be equal or lower than 1. Incision occurs only in the $A_{channel}$ of the cell and the height of terrace ($h_{terrace}$) is recalculated by the following equation:

$$h_{terrace} = \frac{(h_{terrace} - h_{channel}) \cdot (A_{hex} - A_{floodplain})}{(A_{hex} - A_{channel})} \quad \text{(S1.7)}$$

Equation S1.7 is applied in order to maintain only one terrace level within cell. After $h_{terrace}$ is calculated, the variables are updated as follows: $A_{floodplain} = A_{channel}$; $A_{terrace} = A_{hex} - A_{channel}$. After this, $h_{channel}$ is updated following Eq. S1.6, and the volume $q_{sed} - \Delta h_{channel} * A_{channel}$ is transferred to the neighboring cell that receives the sediment and water.

This stage ends after the *Earth surface processes routines* were applied to all cells. Following the flowchart in Figure S2, if a given time (t) in the model isn't the final time (t_f), t is updated with $t + dt$ and the *drainage and lakes calculation routines* will be called again and run using the updated topography. If t is equal or greater than t_f, the model stops and the final topography is saved in a file. Files with the topography in predefined time stages may also be saved if the aim is to analyze the evolution of the model.

S2 WATER DISCHARGE VERSUS SEDIMENT FLUX DATA FOR THE MAIN ALLUVIAL RIVERS IN THE AMAZONIAN LOWLANDS

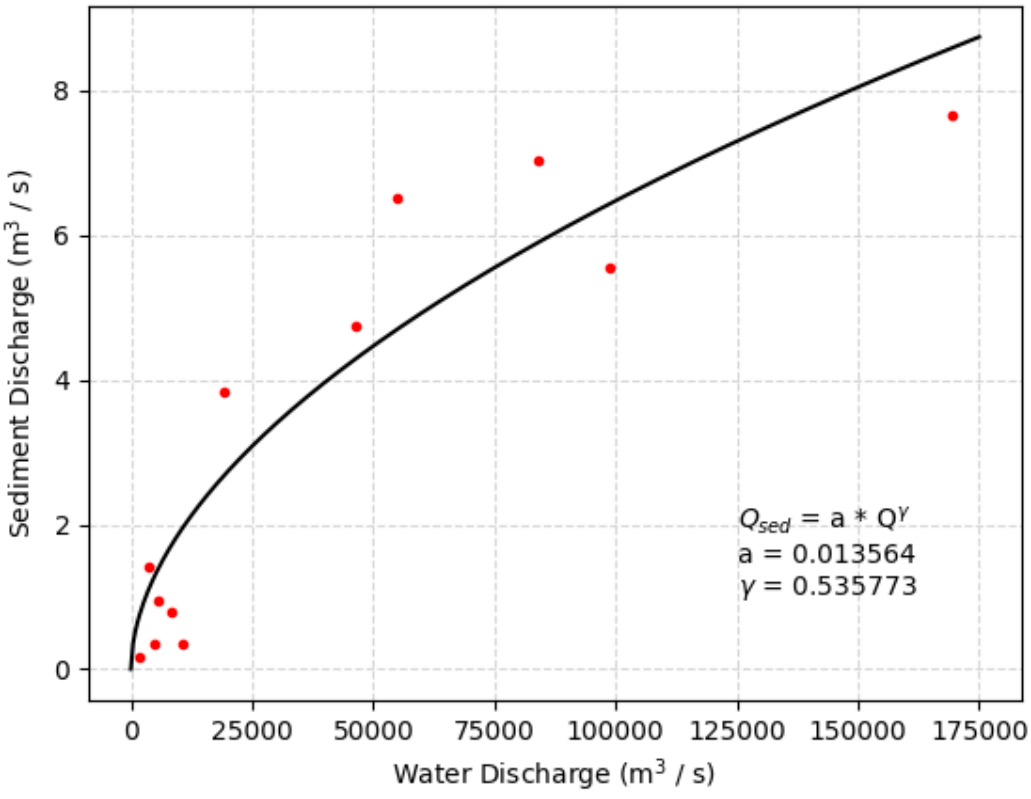

Figure S7 Regression between water discharge versus sediment discharge based on data that has been collected in the main alluvial rivers on the Amazonian lowlands (Filizola and Guyot, 2009). Red dots are the data and the black line is the power function fitted by an ordinary least squares regression.

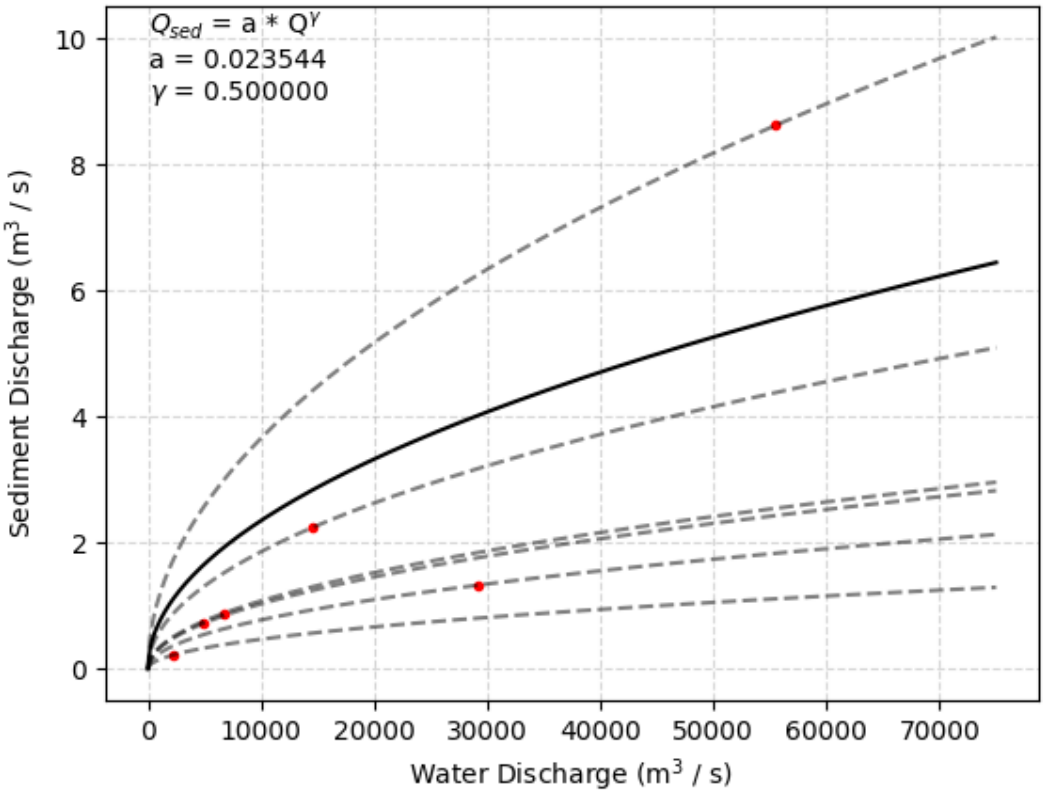

Figure S8 Water discharge versus sediment discharge for the six main rivers entering the grid model. Red dots are the values for each river. Black continuous line is the power function fitted for the data on the image with γ= 0.5. Dashed black lines are the adjustment of Eq. 5 for each river entering the model.

Table S3 Annual mean water discharge, slope and sediment flux used to adjust K_f and m in Eq.1 in the main text. Water discharge and sediment discharge data have been collected in the main alluvial rivers on Amazonian lowlands and are provided by Filizola and Guyot, 2009. Slope estimates are obtained from the SRTM digital elevation model near the gauging stations where the data of Filizola and Guyot, 2009 has been collected.

River	Mean Discharge (m^3 / s)	Slope (m / m)	Sediment flux (m^3 / s)
Javari	640	0.00005	0.01847440055
Solimões	46540	0.00003	4.741578982
Solimões	54940	0.00005	6.523255686
Bia	410	0.00007	0.03694880109
Jurua	910	0.00016	0.1695784528
Jurua	1780	0.00021	0.1624092824
Jurua	4750	0.00012	0.3508757417
Solimões	84010	0.00003	7.029923014
Acre	330	0.00019	0.0580427062
Purus	3650	0.00013	1.415359672
Purus	5520	0.00006	0.9431595085
Purus	10720	0.00008	0.3398462489
Solimões	98750	0.00002	5.552660314
Guaporé	60	0.00017	0.001240817947
Guaporé	530	0.00006	0.003308847859
Guaporé	910	0.00009	0.001930161251
Mamoré	8400	0.00008	0.7782685902
Madeira	19360	0.00005	3.8255796
Amazonas	169480	0.00001	7.66453246

S3 EXAMPLES SHOWING LANDSCAPE RESPONSE IF DIFFERENT VALUE FOR LATERAL EROSION COEFFICIENT ARE USED

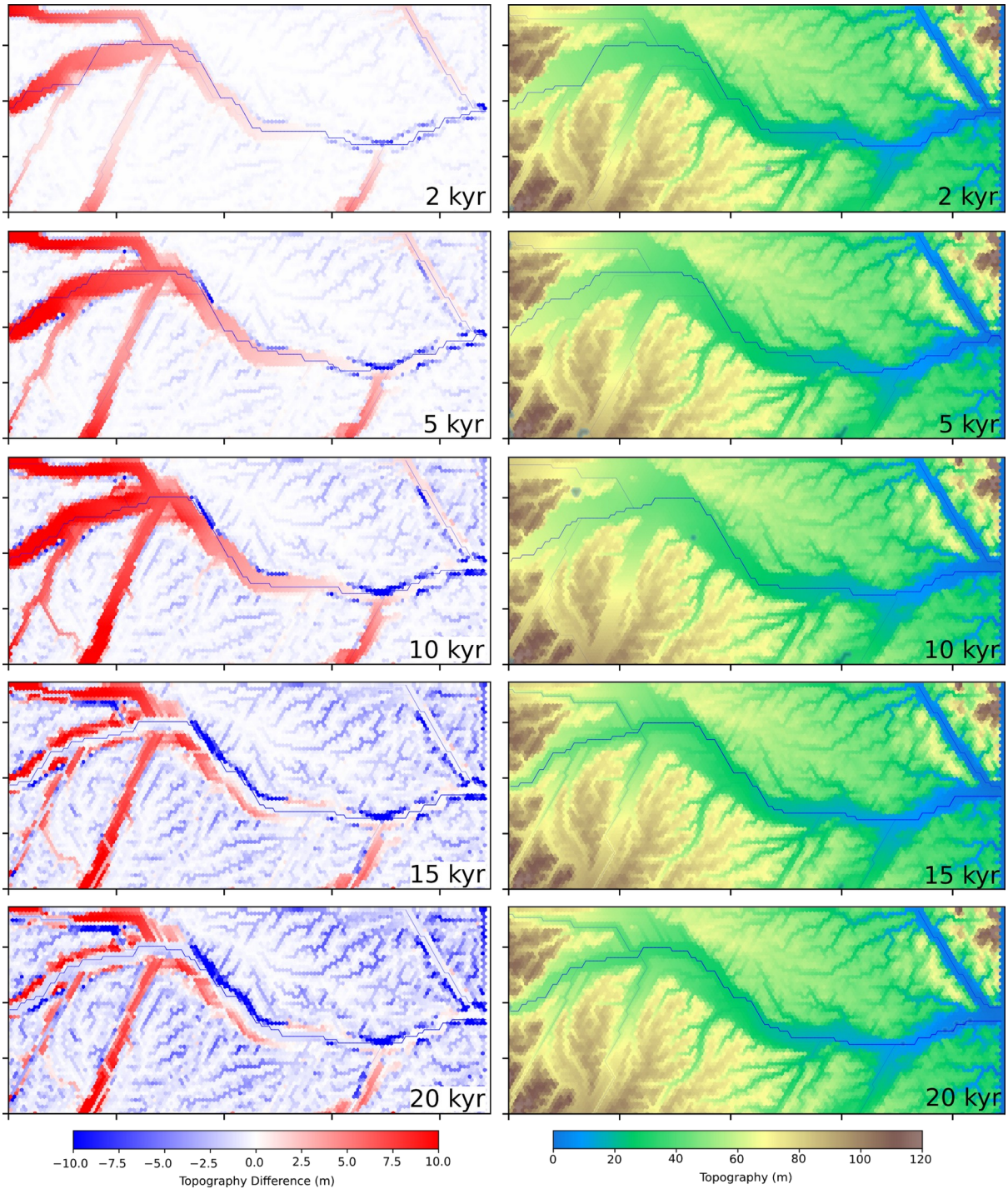

Figure S9 Landscape evolution with lateral erosion coefficient α_1 equal to 6.3 (Eq. 4 at the main text). The water input is 30 % less than the current water input (dryer period) during the first 10 ky and then increases to the current water input until 20 ky. **Left figures** show the difference of the topography in relation to the initial topography, with colours saturated in red for values above 10 m and in blue for values below - 10 m. **The right figures** show the topography itself. The occasional blue stains on the map represent lakes (Local minima).

Accordingly, low values of lateral erosion yields poorly developed floodplains, but in good preservation of the mid-lower terraces.

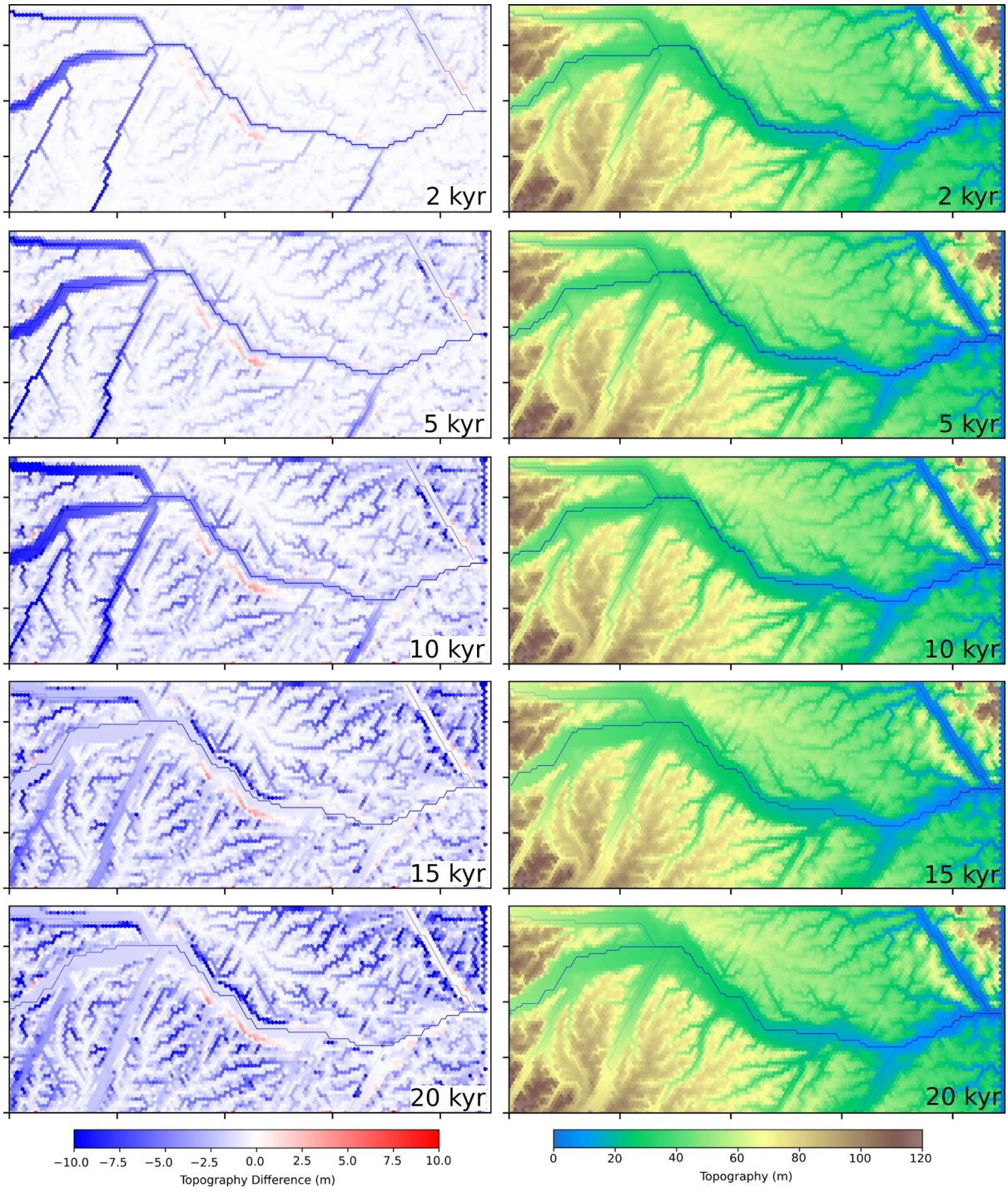

Figure S10 Landscape evolution with lateral erosion coefficient α_1 equal to 6.3 (Eq. 4 at the main text). The water input is 30 % higher than the current water input (dryer period) during the first 10 ky and then back to current water input until 20 ky. Accordingly, low lateral erosion also yields poorly developed floodplains, but few mid-lower terraces because of the wet-to-dry climate change scenario.

S4 EXAMPLES SHOWING ALTERNATIVE PRECIPITATION CONDITIONS

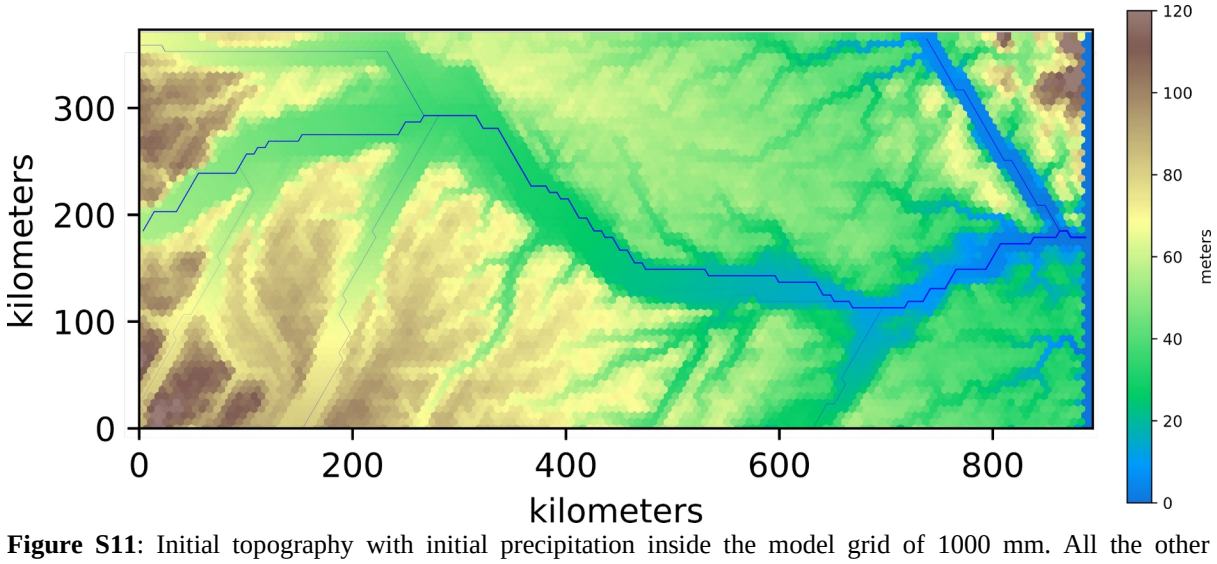

Figure S11: Initial topography with initial precipitation inside the model grid of 1000 mm. All the other parameters are equivalent to the tested scenario in the main text. The blue lines represent the channels and the thickness of the line is proportional to the discharge of the corresponding stream. The names of the rivers outside of the grid are indicated. The base level is controlled by the elevation of the sink cells locked at 0 m and located on the last right column of the grid.

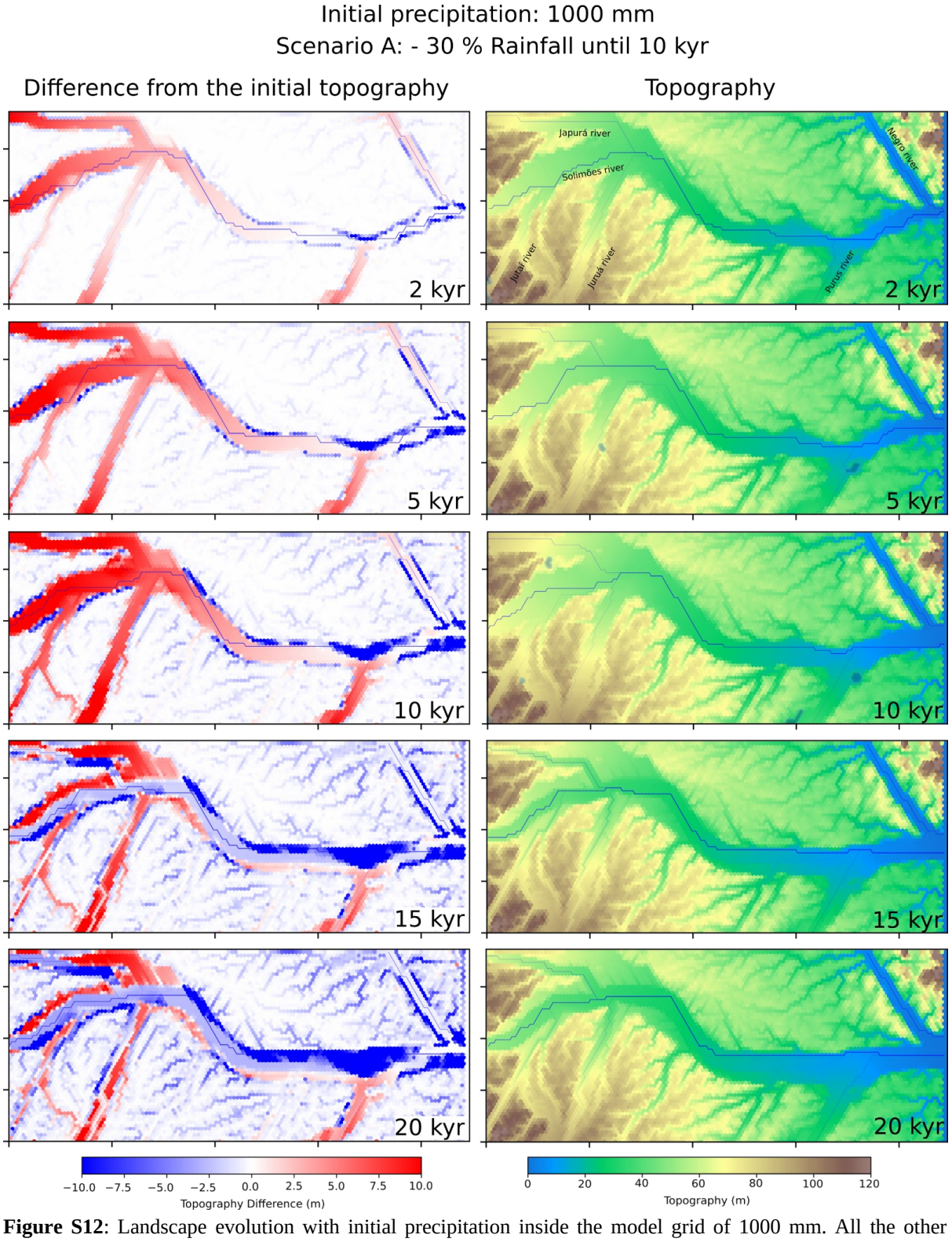

Figure S12: Landscape evolution with initial precipitation inside the model grid of 1000 mm. All the other parameters are equivalent to the tested scenario in the main text. The water input is 30 % less than the current water input (dryer period) during the first 10 kyr and then increases to the current water input until 20 kyr.

300

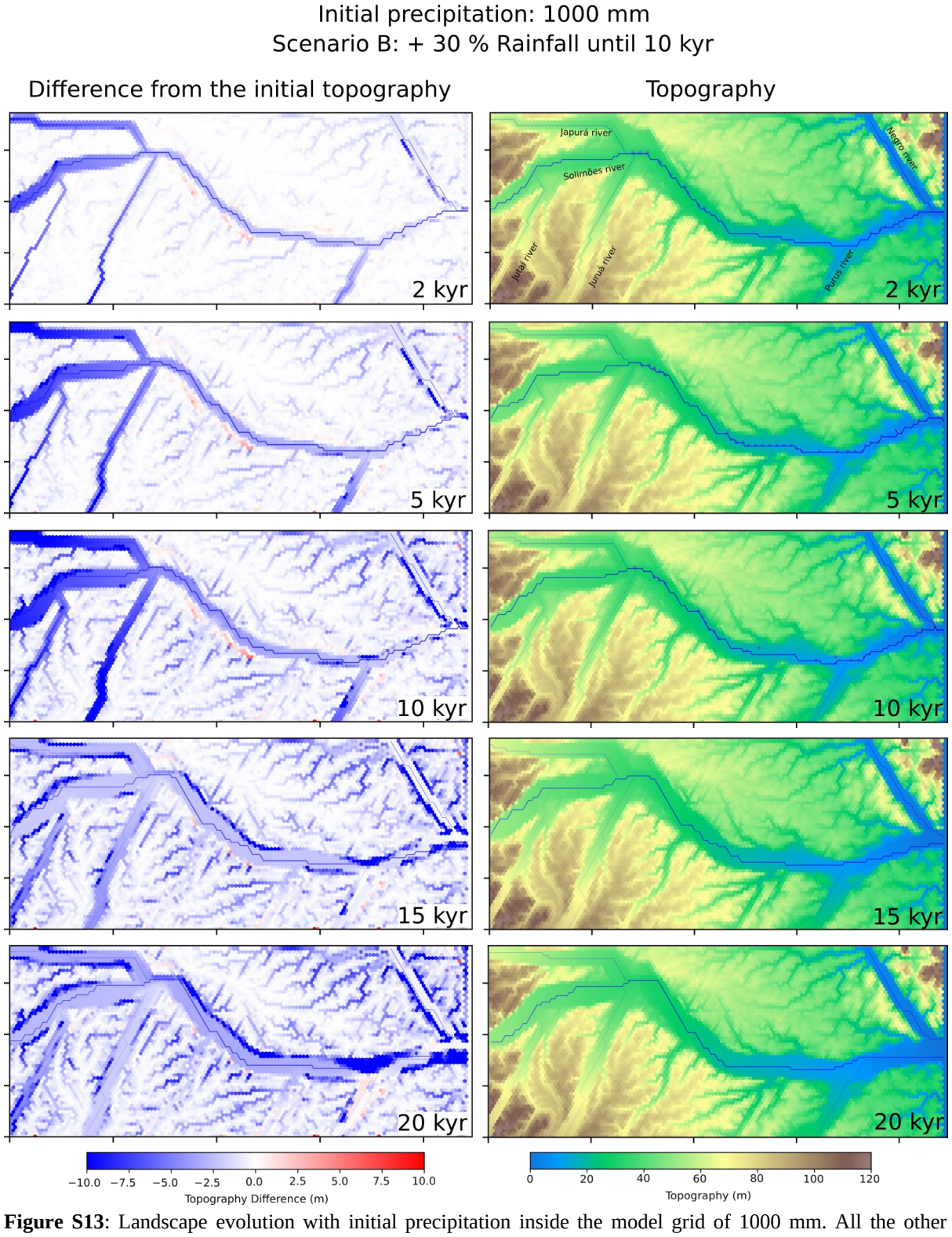

Figure S13: Landscape evolution with initial precipitation inside the model grid of 1000 mm. All the other parameters are equivalent to the tested scenario in the main text. The water input is 30 % higher than the current water input (dryer period) during the first 10 kyr and then back to current water input until 20 kyr.

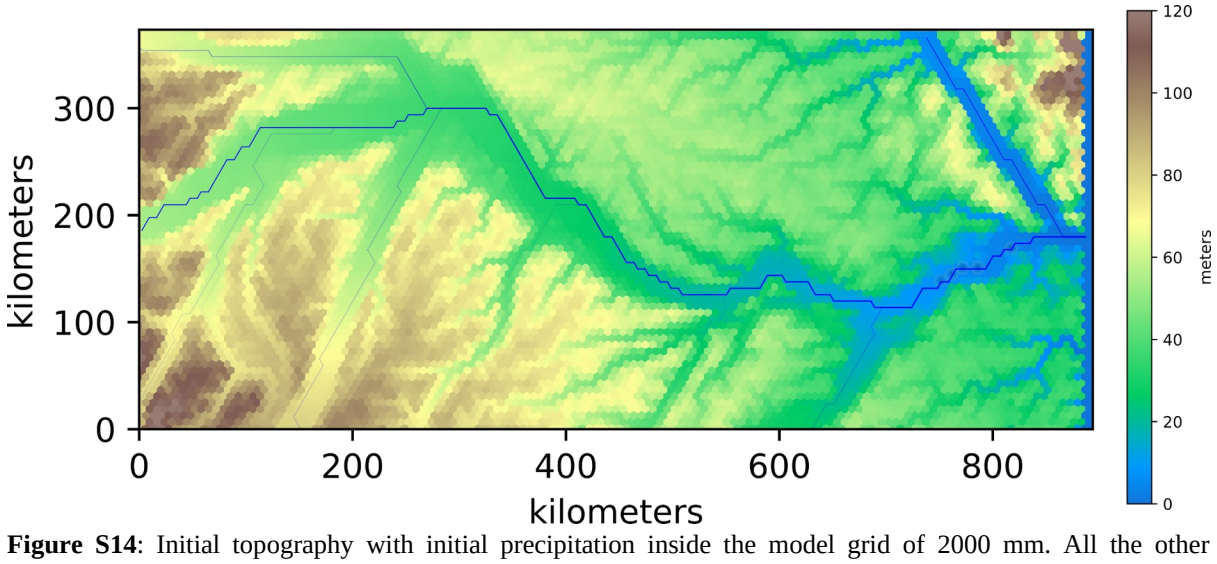

Figure S14: Initial topography with initial precipitation inside the model grid of 2000 mm. All the other parameters are equivalent to the tested scenario in the main text.

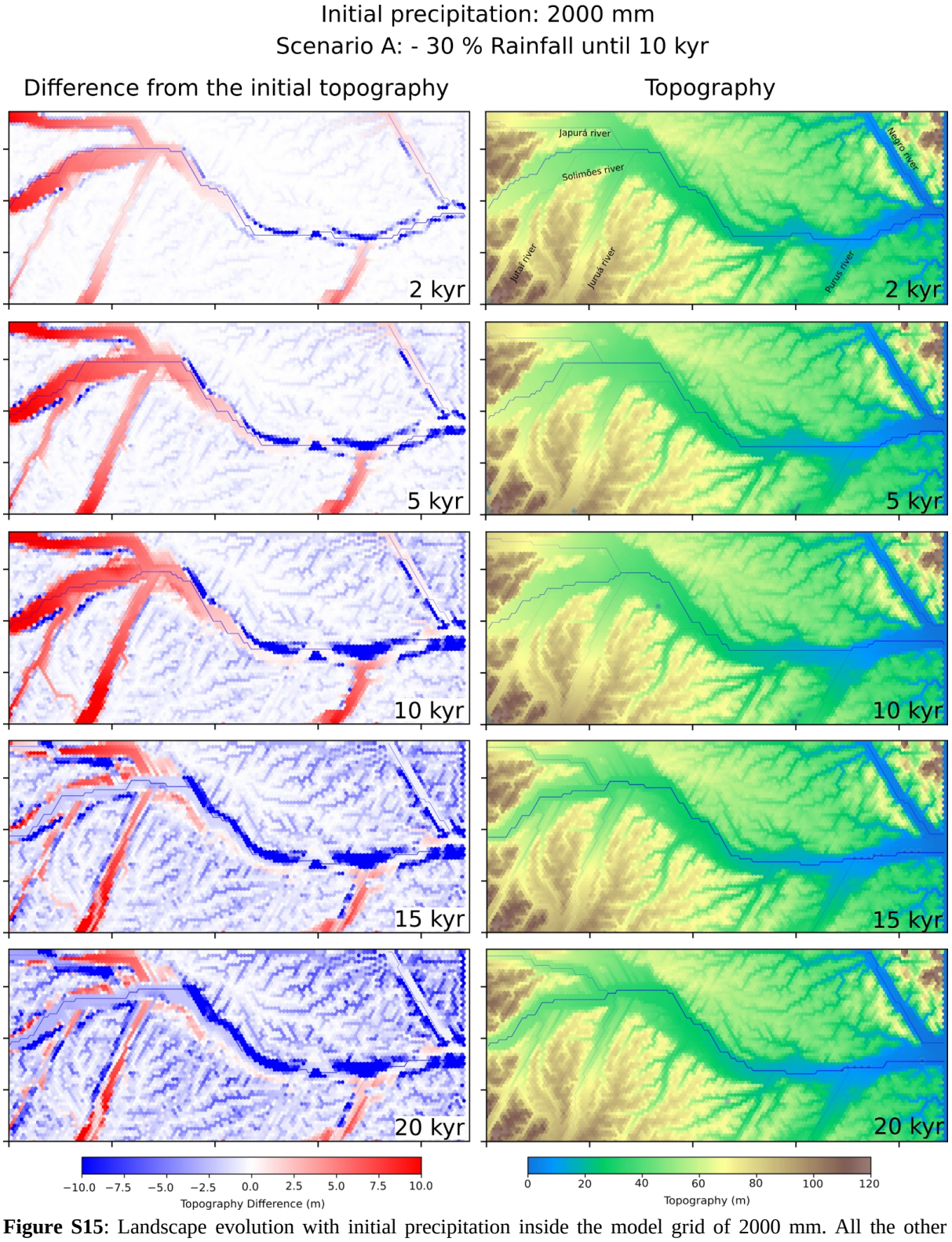

Figure S15: Landscape evolution with initial precipitation inside the model grid of 2000 mm. All the other parameters are equivalent to the tested scenario in the main text. The water input is 30 % less than the current water input (dryer period) during the first 10 kyr and then increases to the current water input until 20 kyr.

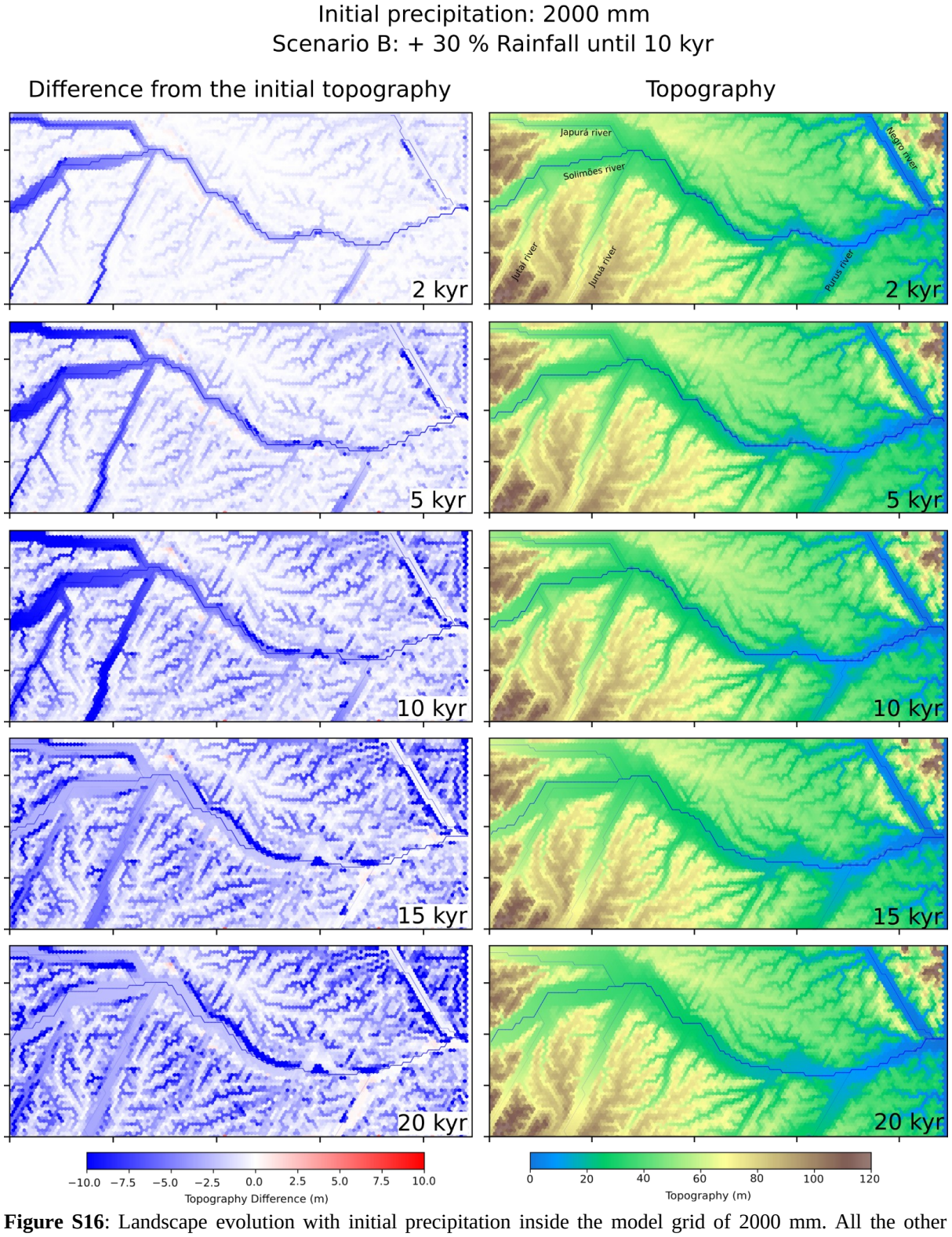

315 **Figure S16**: Landscape evolution with initial precipitation inside the model grid of 2000 mm. All the other parameters are equivalent to the tested scenario in the main text. The water input is 30 % higher than the current water input (dryer period) during the first 10 kyr and then back to current water input until 20 kyr.

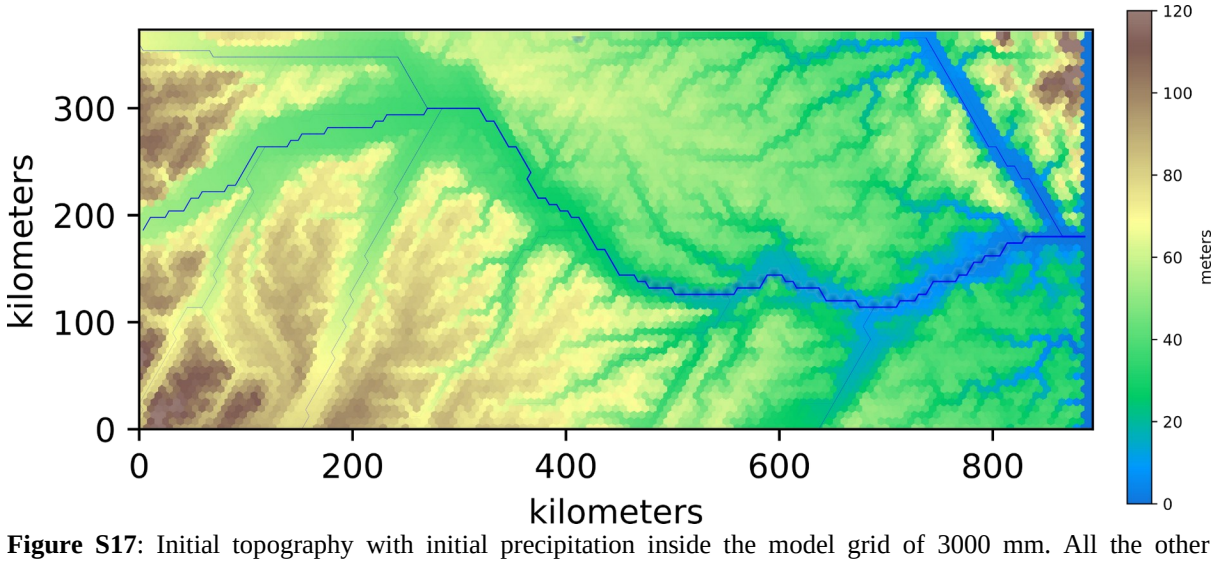

Figure S17: Initial topography with initial precipitation inside the model grid of 3000 mm. All the other parameters are equivalent to the tested scenario in the main text.

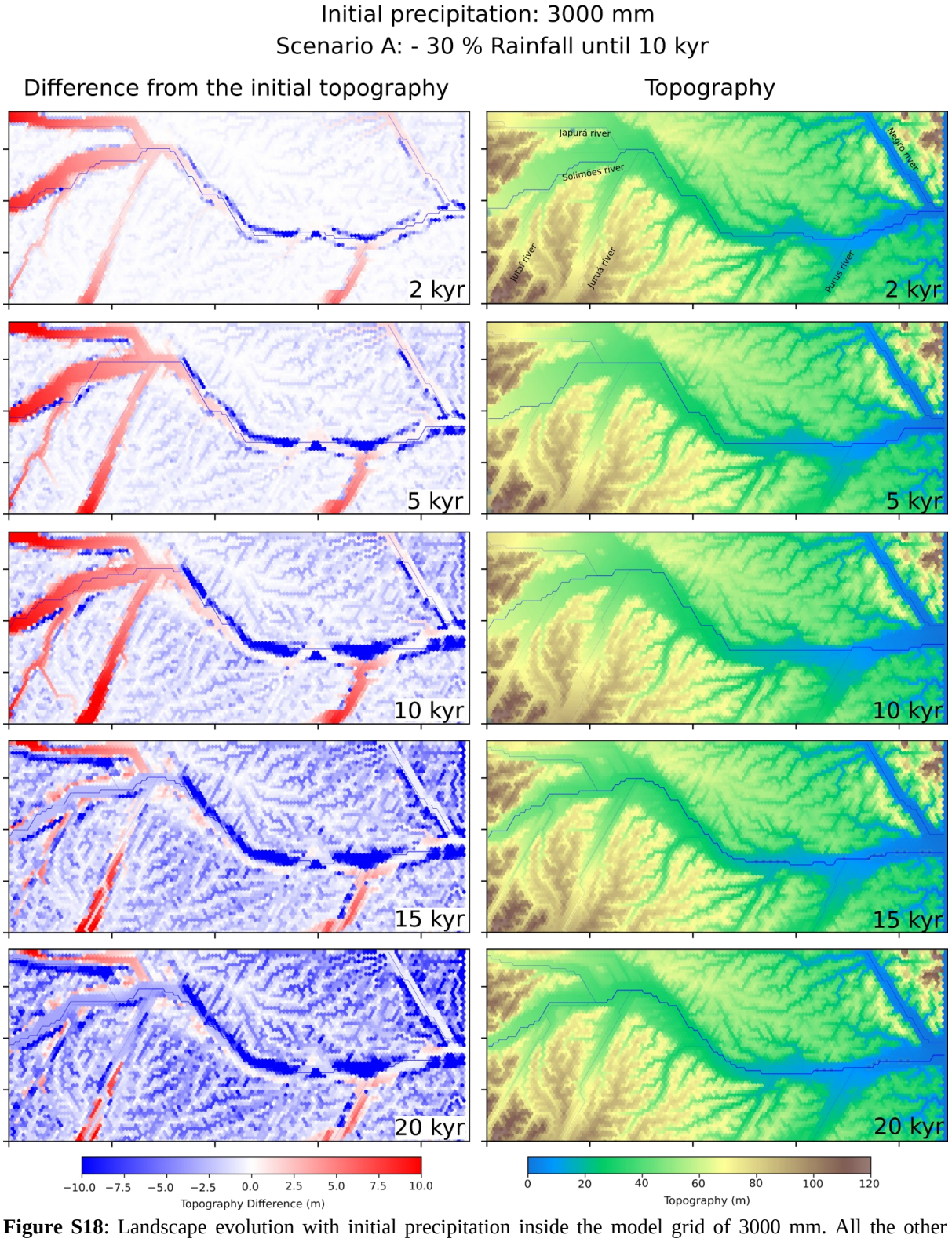

Figure S18: Landscape evolution with initial precipitation inside the model grid of 3000 mm. All the other parameters are equivalent to the tested scenario in the main text. The water input is 30 % less than the current water input (dryer period) during the first 10 kyr and then increases to the current water input until 20 kyr.

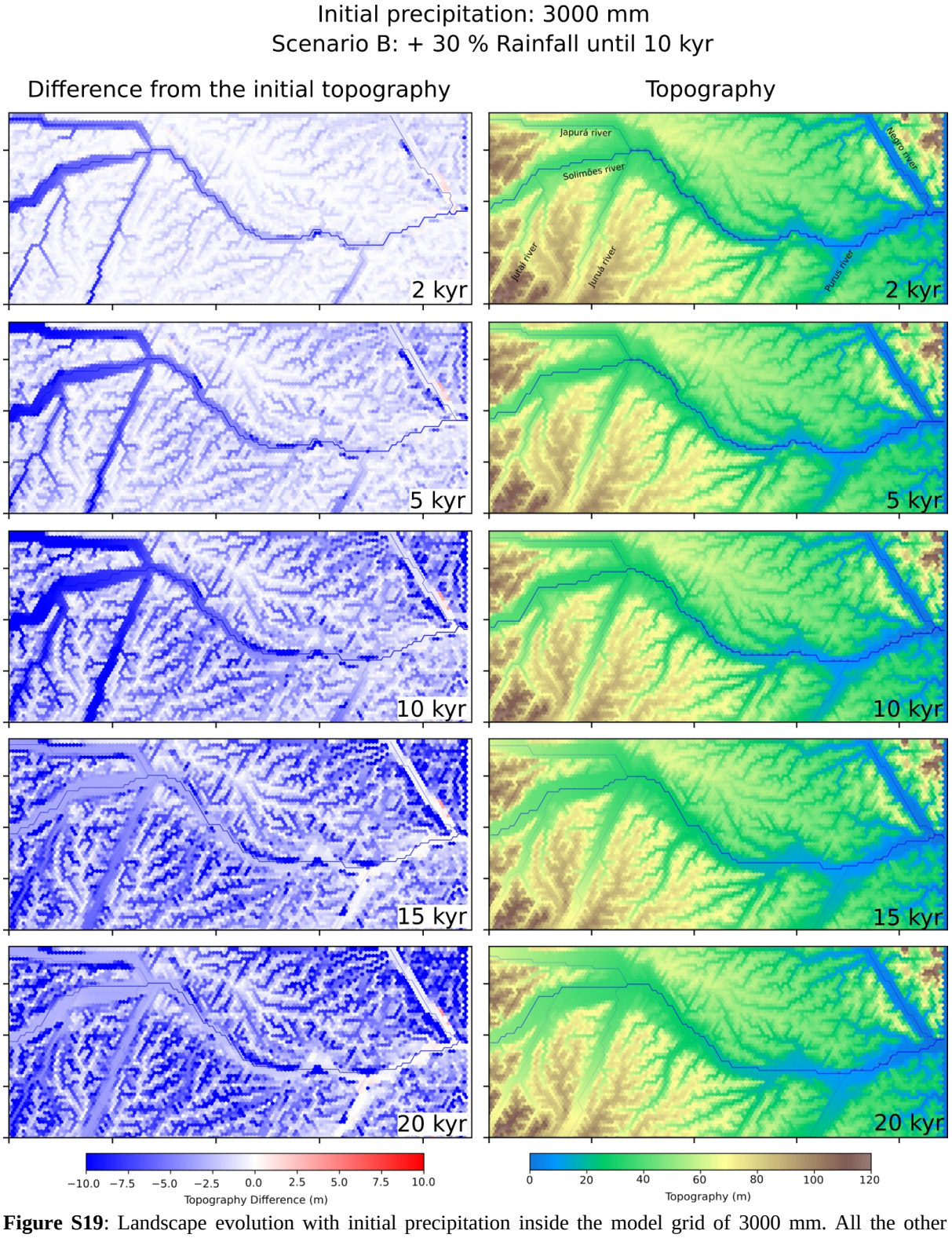

Figure S19: Landscape evolution with initial precipitation inside the model grid of 3000 mm. All the other parameters are equivalent to the tested scenario in the main text. The water input is 30 % higher than the current water input (dryer period) during the first 10 kyr and then back to current water input until 20 kyr.

S5 SUPPLEMENT REFERENCES

Beaumont, C., Fullsack, P. Hamilton, J., 1992, Erosional control of active compressional orogens, *in* McClay, K.R. , ed., Thrust Tectonics: London, Springer-Science+Business Media, B.V., p. 1–18., doi:10.1007/978-94-011-3066-0.

Braun, J., Sambridge, M., 1997, Modelling landscape evolution on geological time scales: a new method based on irregular spatial discretization: Basin Research, v. 9, p. 27–52, doi: 10.1046/j.1365-2117.1997.00030.x.

Espinoza JC, Ronchail J, Guyot JL, Cochonneau G, Filizola N, Lavado W, Oliveira E, Pombosa R, Vauchel P (2009a) Spatio-Temporal rainfall variability in the Amazon Basin Countries (Brazil, Peru, Bolivia, Colombia and Ecuador). Int Jour of Clim, 29, 1574-1594.

Filizola, N., Guyot, J.L., 2009, Suspended sediment yields in the Amazon basin: an assessment using the Brazilian national data set: Hydrological Processes, v. 23, p. 3207-3215.

Guimberteau, M., Ronchail, J., Espinoza, J.C., Lengaigne, M., Sultan, B., Polcher, J., Drapeau, G., Guyot, J.L., Ducharne, A., Cialis, P., 2013, Future changes in precipitation and impacts on extreme streamflow over Amazonian sub-basins: Environmental Research Letters, v. 8, p. 1-13, doi: 10.1088/1748-9326/8/1/014035.

Moody, J., and B. Troutman (2002), Characterization of the spatial variability of channel morphology, Earth Surf. Processes Landforms, 27(12), 1251–1266.

Sacek, V., 2014, Drainage reversal of the amazon river due to the coupling of surface and lithospheric processes: Earth and Planetary Science Letters, v. 401, Supplement C, p. 301–312, doi: 10.1016/j.epsl.2014.06.022.

Van De Wiel, M.J., Coulthard, T.J., Macklin, M.G., Lewin, J., 2007, Embedding reach-scale fluvial dynamics within the CAESAR cellular automaton landscape evolution model: Geomorphology, v. 90, p. 283–301, doi: 10.1016/j.geomorph.2006.10.024.